Available online at www.sciencedirect.com

ScienceDirect

Procedia Structural Integrity 35 (2022) 34–41

Structural Integrity Procedia

www.elsevier.com/locate/procedia

2nd International Workshop on Plasticity, Damage and Fracture of Engineering Materials

A Two-Level Homogenization Approach for Polymer Nanocomposites with Coated Inclusions

Dilek Güzel[a,b,*], Ercan Gürses[a]

[a]*Middle East Technical University, Department of Aerospace Engineering, Ankara 06800, Turkey*
[b]*TU Dortmund, Institute of Mechanics, Dortmund 44227, Germany*

Abstract

In polymer nanocomposites, other than the matrix and inclusion, a third phase so-called interphase, is commonly observed. Interphase properties affect the overall macroscopic mechanical behavior. It is crucial to model the interphase and obtain the effective composite properties accordingly. Homogenization theory is very useful and powerful; however, many of the homogenization-based techniques have deficiencies. The goal of the study is to combine two very well-known homogenization techniques to model the polymer nanocomposites with coated inclusions. One of the goals of the study is to demonstrate the deficiency that originated from the interphase modeling and overcome this problem by the proposed two-level homogenization method. This method aims to model load transfer between the matrix and the reinforcement element through the interphase in a correctly. For this purpose, first, an effective inclusion is formed using finite element homogenization, then the effective inclusion and the matrix are homogenized using micromechanics-based Double Inclusion method. The proposed method provides a remarkable improvement compared to the micromechanics-based method for the soft interphase case.

Keywords: polymer nanocomposites, homogenization theory, interphase, micromechanics

1. Introduction

Polymer nanocomposites are materials that have polymer matrices and nano-scale reinforcement elements. Unlike classical, conventional composites, nanocomposites exhibit some phenomena that can be explained by the nano-scale nature of the material (Bhattacharya et al. (2008)). Therefore, new theoretical principles and different experimental techniques are needed to understand the behavior of nanocomposites. Today, many experimental and numerical works on polymer nanocomposites are present in the literature. The effect of matrix and reinforcement element's properties, size, shape, distribution, and different production techniques and conditions have been studied and reported extensively. Other than the matrix and the reinforcement element, another phase in nanocomposite systems has been

* Güzel D. Tel.: +49-231-755-5790
E-mail address: dilek.guezel@tu-dortmund.de

10.1016/j.prostr.2021.12.045

observed. Some of the property enhancement or deficiency has been attributed to the third phase, known as the interphase. Interphase's characterization and understanding of the behavior became very important in nanocomposite research.

The properties of the interphase region significantly affect the performance of the composite material. The establishment of weak or strong interface interactions between the polymer matrix and the inclusion affects the composite's behavior; hence it should be considered when modeling the composite. Some properties of the interphase can be obtained experimentally, see, e.g., Brune et al. (2016), Tian et al. (2019) or by molecular dynamics and similar simulation methods, see, e.g., Odegard et al. (2005). In modeling the macroscopic behavior of nanocomposite materials, it has become necessary to investigate the general structure and properties of the interphase region.

There are different approaches in the literature for modeling the interphase and analyzing the effect of the interphase properties on the macroscopic behavior of the composite. The proposed method is based on evaluating the interphase as a coated region or a layer around the inclusion. This approach, which is used to estimate effective elastic moduli of multi-phase composites, considers the interactions between the phases during the heterogeneous medium's homogenization. These approaches are known in the literature as the *coated inclusion problem*.

The Composite Sphere Assemblage model was proposed in 1962 in Hashin (1962) to determine the effective mechanical properties of the n-phase heterogeneous environment. The Composite Sphere Assemblage is based on the well-known analytical results of Eshelby (1957). It is a method used to determine the limits of bulk and shear moduli of spherical and cylindrical inclusion problems. Benveniste et al. (1989) introduced a micromechanics-based approach using the *average stress in the matrix* concept developed by Mori and Tanaka (1973). Since for high inclusion volume fractions the Mori-Tanaka model does not work properly, another micromechanics-based approach known as the Generalized Self-Consistent Scheme (GSCS) is developed, see Herve and Zaoui (1993); Christensen and Lo (1979). In this method, the phase that creates heterogeneity is assumed to be embedded in an environment with effective composite properties. By means of an iterative algorithm, effective elastic properties of the composite can be estimated. In 1993, the Double-Inclusion model was presented by Hori and Nemat-Nasser (1993). The Double-Inclusion model is one of the most well-known, accepted, and implemented methods by date. This model deals with the general case of coated ellipsoidal inclusions in an anisotropic medium in which the inter-inclusion interaction is also evaluated. However, the simplifying assumption of a uniform strain field inside the coating is still accepted.

The paper is organized as follows. In section 2, in order to utilize the proposed two-level homogenization technique, the Double-Inclusion model and strain-controlled tests by finite element analysis are presented. The proposed method and the necessity of a two-level homogenization technique in the soft interphase case are demonstrated and different comparisons for two-dimensional (circular) and three-dimensional (spherical) geometries are illustrated in section 3. Finally, the conclusions and the outlook are presented in section 4.

2. Method

In 2006, Friebel et al. (2006) proposed two new techniques, two-level, and two-step homogenization, for the general solution to the coated inclusion problem. The two-level approach is based on the matrix seeing the inclusion and surrounding coating region as a composite structure. Generally, two-level homogenization methods have a replacement procedure at the first level of homogenization. At the first level, the coated inclusion is treated as a two-phase composite and is homogenized using different methods. At the end of the first level, the new effective inclusion is placed inside the matrix, then at the second level, the matrix and the effective inclusion can be homogenized to model the overall effective composite behavior. Different researchers have implemented two-level homogenization schemes as a common practice, see Chatzigeorgiou et al. (2012), Shajari et al. (2018).

2.1. Double-Inclusion model

In this work, the Double-Inclusion (D-I) model, proposed by Hori and Nemat-Nasser (1993), is used for the proposed homogenization technique and comparison purposes. In the micromechanics-based model, the inclusions and coating phases are assumed to be ellipsoidal. Also, the inclusion and the coating are assumed to be coaxial. The D-I model is not limited to isotropy; elastic phases can be anisotropic or isotropic. The elasticity tensor of a multi-phase composite $\mathbb{C}$ is given in (1).

$$\mathbb{C} = \mathbb{C}^{inf} : [\mathbb{I} + (\mathbb{S} - \mathbb{I}) : \mathbf{\Lambda}] : [\mathbb{I} + \mathbb{S}\mathbf{\Lambda}]^{-1} \tag{1}$$

where ϕ_i is the volume fraction of i^{th} phase, $\mathbb{C}^{inf}$ is the elasticity tensor of an infinitely extended homogeneous domain, $\mathbb{I}$ is the fourth-order identity tensor, $\mathbb{S}$ is the Eshelby tensor for ellipsoidal inclusion of Eshelby (1957).

The parameter $\mathbf{\Lambda}$ in (1) should be evaluated for every phase (n-phase). If the elasticity tensor is uniform in each phase, Λ can be expressed as in (2). The D-I model allows the phases to be non-uniform for graded evolution of any of the phases, see Li (2000). In (2), $\mathbb{C}_i$ corresponds to the elasticity tensor of the phases. Some remarks should be made at this point: the elasticity tensor of an infinitely extended homogeneous domain, $\mathbb{C}^{inf}$ has an initial, arbitrary value; since this is an iterative procedure, at every step, this tensor should be updated until the convergence is achieved.

$$\mathbf{\Lambda} = \sum_{i=1}^{n} \phi_i \Lambda_i \quad \Lambda_i = [(\mathbb{C}^{inf} - \mathbb{C}_i)^{-1} : \mathbb{C}^{inf} - \mathbb{S}]^{-1} \tag{2}$$

In two-dimensional analyses, some modifications are needed in the formulation of the micromechanics-based D-I model. First of all, the volume fraction is defined differently in two- and three-dimensions, as can be seen in (3). A_i and V_i correspond to the area and the volume of the i^{th} phase. Thus, for spherical and circular geometries, both of these definitions depend on the radius (r_i) of the phase

$$\phi_i^{2d} = \frac{A_i}{\sum_{i=1}^{n} A_i} = \frac{r_i^2}{\sum_{i=1}^{n} r_i^2} \quad \phi_i^{3d} = \frac{V_i}{\sum_{i=1}^{n} V_i} = \frac{r_i^3}{\sum_{i=1}^{n} r_i^3} \quad . \tag{3}$$

The Eshelby tensor $\mathbb{S}$ is not updated for two-dimensional problems. However, in order to use the Eshelby tensor in two dimensions, aspect ratio information is changed to [1 1 ∞]. Normally for a spherical particle, the aspect ratio is set as [1 1 1]. Two radii are equal, and the last one should be a very high value for a circular inclusion in two-dimensional problems. It seems like it is a cylinder, and a cut in the $x - y$ plane is obtained.

2.2. Homogenization with finite element method

For a heterogeneous medium, when the balance of linear momentum, boundary conditions and the constitutive equations are considered, stress and strain fields are expected to be oscillatory due to heterogeneity of the microstructure. In such complex problems, the homogenization method provides a simple solution for effective material behavior. In this study, strain-controlled tests (FE simulations) are conducted, and uniform displacement boundary conditions are applied to the representative volume element (RVE). After obtaining the homogenized stress and strain tensors, effective properties can be obtained.

For the most general case of anisotropic linear elasticity, the elasticity tensor $\mathbb{C}$ has 81 components (21 of which are independent). Thus, 21 equations are needed to obtain 21 constants. Macroscopic stress tensors are calculated by performing strain-controlled finite element analyses. In order to determine each column of the elasticity matrix, only one component of the strain tensor is specified to a non-zero value while all the other components are set to zero. The elasticity tensor is computed by conducting finite element analyses of the six load cases given in (4)

$$\bar{\boldsymbol{\epsilon}} = \begin{bmatrix} a & 0 & 0 \\ 0 & 0 & 0 \\ 0 & 0 & 0 \end{bmatrix}, \quad \begin{bmatrix} 0 & 0 & 0 \\ 0 & a & 0 \\ 0 & 0 & 0 \end{bmatrix}, \quad \begin{bmatrix} 0 & 0 & 0 \\ 0 & 0 & 0 \\ 0 & 0 & a \end{bmatrix}, \quad \begin{bmatrix} 0 & a & 0 \\ a & 0 & 0 \\ 0 & 0 & 0 \end{bmatrix}, \quad \begin{bmatrix} 0 & 0 & 0 \\ 0 & 0 & a \\ 0 & a & 0 \end{bmatrix}, \quad \begin{bmatrix} 0 & 0 & a \\ 0 & 0 & 0 \\ a & 0 & 0 \end{bmatrix} \tag{4}$$

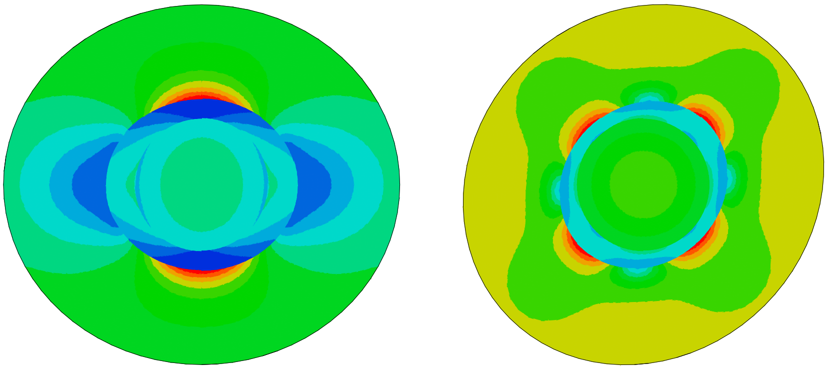

(a) Uniaxial tension test

(b) Simple shear test

Fig. 1: Deformed views of the RVEs for the uniaxial test in x-direction and thesimple shear in $x-y$ plane. The contours correspond to the magnitude of the von Mises stress

where a is a small constant taken as 0.05 in computations. In (4), the first three load cases correspond to the uniaxial loading, while the last three correspond to the simple shear loading. Fig. 1a shows von Mises stress distribution and the deformed shape of the spherical volume element under uniaxial loading in $x-$ direction. Fig. 1b shows the deformed shape of the spherical volume element when subjected to a simple shear in the $x-y$ plane. Note that, since the behavior is assumed to be linear elastic, the value of a does not affect the homogenized moduli computed.

In the current study, spherical RVEs with spherical inclusions and circular RVEs with circular inclusions are considered. Abaqus/Standard is used for the finite element analyses ABAQUS (2009). The geometry, load conditions, and boundary conditions are created in Abaqus. In Fig. 2a, a cut-out image of the RVE is shown where the gray part is the matrix, while red is the interphase and black is the inclusion. The corresponding two-dimensional view of the mesh is illustrated in Fig. 2b. As seen in Fig. 2b, a structured mesh is used. A linear, 8-node brick element (C3D8) with full integration is chosen for three-dimensional analyses. A 4-node bilinear, plane strain, quadrilateral element (CPE4) with full integration is utilized for two-dimensional analyses. A 4-node plane stress quadrilateral element (CPS4) is also utilized to compare the plane strain and plane stress cases.

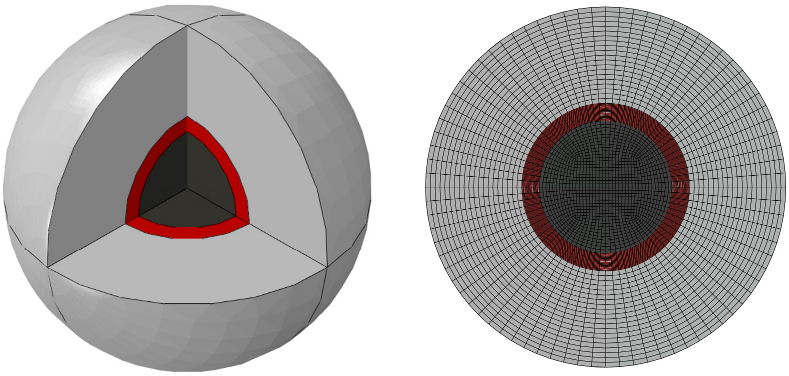

(a) Three-dimensional spherical RVE

(b) Two-dimensional circular RVE

Fig. 2: The spherical representative volume element and the corresponding finite element mesh for coated inclusion problem

After applying a load case to the RVE, the homogenized stress tensor is computed. Since a uniform displacement boundary condition is applied to the entire surface of the RVE, the homogenized strain tensor is prescribed. The volume of each integration point is also stored during the finite element analysis of the RVE. Using a simple Python code, the homogenized stress and strain tensors are computed with the help of the stress and strain tensors at the integration points, which is depicted in (5).

$$\bar{\boldsymbol{\sigma}} = \frac{\sum_{i=1}^{\mathrm{NIP}} \boldsymbol{\sigma}_i V_i}{\sum_{j=1}^{\mathrm{NIP}} V_j} \qquad \bar{\boldsymbol{\epsilon}} = \frac{\sum_{i=1}^{\mathrm{NIP}} \boldsymbol{\epsilon}_i V_i}{\sum_{j=1}^{\mathrm{NIP}} V_j} \tag{5}$$

In (5), $\boldsymbol{\sigma}_i$ and $\boldsymbol{\epsilon}_i$ correspond to the stress and the strain tensors at the integration point i, V_i is the volume of that integration point, and NIP is the total number of integration points of the FE model.

Periodic boundary condition (PBC) is commonly utilized in homogenization problems. Since a circular RVE is not space-filling, uniform displacement boundary condition is employed in proposed framework. Firooz et al. (2019) demonstrated that for a circular RVE uniform displacement and periodic boundary conditions render the same results for effective material properties. The proposed methodology in this article uses a two-level homogenization technique. Forming an *effective inclusion* is the main goal at the first level. Then, any homogenization technique can be used in the second level to homogenize the obtained two-phase composite. This study proposes a two-level technique based on micromechanics and FEA, and the results are reported for linear elastic material behavior. The proposed method can be utilized even if constituents are anisotropic or the macroscopic response is anisotropic due to the shape of inclusion. For non-spherical inclusions reader may refer to Güzel (2021).

3. Results

3.1. Comparison of double-inclusion model and the proposed methodology

An important aspect of the Double-Inclusion method is related to the interactions between different inclusions and between the inclusion and surrounding coating phase. The D-I model uses a strain concentration tensor approach, and these interactions are taken into account. However, the fact that the interphase surrounds the inclusion is not taken into account properly. In the D-I model, analytical estimates of a nested ellipsoidal geometry were reported by Hori and Nemat-Nasser (1993). This specific geometry definition provides stress and strain fields for inclusions to be affected by this nested structure. However, it was pointed out by Wang et al. (2016), when the aspect ratios of the inclusion and the coating are the same, the D-I model becomes equivalent to the Mori-Tanaka method. This is shown analytically for spherical inclusions Wang et al. (2016). This result implies that the D-I model does not see the interphase as a coating region around the inclusion, but the D-I model sees it as a different filler phase with interphase properties. Therefore, the stress transfer between phases due to nested structure cannot be modeled using the D-I model. In the D-I model, the coating phase behaves as it was a separate phase in the matrix. This deficiency is expected to be significant, particularly when the interphase is soft.

Table 1: Material properties for the composite system

Material	Young's modulus E[GPa]	Poisson ratio $\nu[-]$
Matrix	2.5	0.34
Interphase	0.25 or 25.0	0.30
Inclusion	1000	0.30

Two cases are studied, namely, the interphase being softer than the matrix and the interphase being stiffer than the matrix. The corresponding Young's modulus for the soft and the stiff interphases are $0.1 \times E_m = 0.25$GPa and $10 \times E_m = 25$GPa. For both cases, $\nu = 0.3$ is chosen. In the micromechanics-based model proposed by Hori and Nemat-Nasser (1993), the inclusions and coating phases are assumed to be ellipsoidal. Also, the inclusion and the coating are assumed to be coaxial.

Fig. 3a proves that when there is stiff interphase, the micromechanics-based model is in a good agreement with the three-phase FEA (reference solution). However, when the interphase is softer than the matrix, these models do not match. The D-I model even shows an increasing trend for high volume fractions while the reference solution is monotonously decreasing. It shows that, even though the volume fraction of inclusion increases, the overall macroscopic elastic modulus decreases due to soft interphase. Therefore, even the trend of the elastic modulus with the volume fraction is different for the D-I model and the reference FE solution. In order to overcome the stress shielding

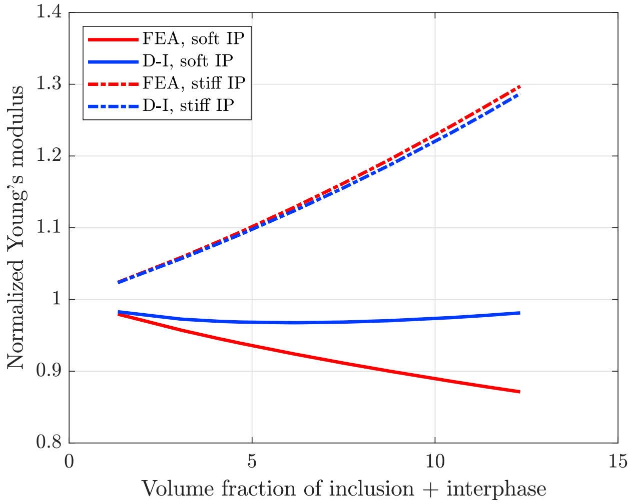

(a) Three-dimensional D-I and FEA comparison

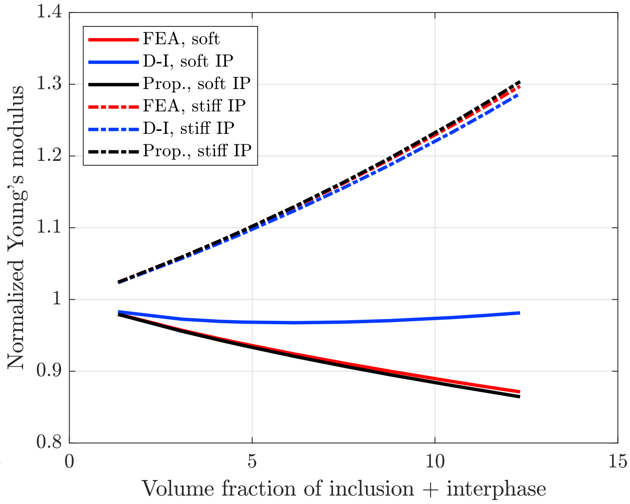

(b) Three-dimensional comparison of proposed method

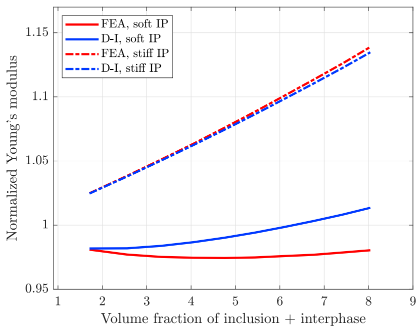

(c) Two-dimensional D-I and FEA comparison

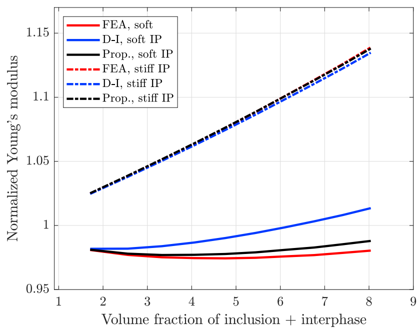

(d) Two-dimensional comparison of proposed method

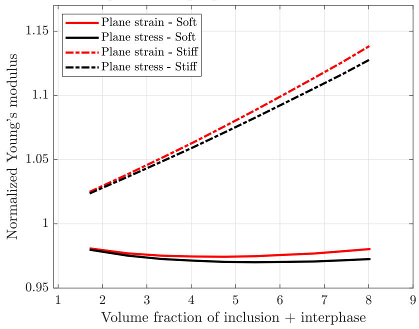

(e) Effective Young's modulus comparison as a reference solution for plane strain and plane stress condition

Fig. 3: Reference results for two- and three-dimensional problems

problem for soft interphase and eliminate this mismatch, proposed method is also used for three-dimensional geometries as well. The comparison of the proposed method with the D-I method and the reference solution is given in Fig. 3b. The predictions of the proposed method are closer to the reference solution for the stiff interphase case as well.

In three-dimensional models, all the phases are assumed to be isotropic. In two-dimensional problems, in addition to isotropy, plane strain and plane stress assumptions are considered to see how these assumptions affect the overall effective elastic modulus. Fig. 3e demonstrates that the elastic moduli for plane strain and plane stress conditions are not the same, while they seem very close for lower volume fractions. The plane strain effective moduli both for the soft and the stiff interphase are higher than the plane stress moduli. However, the results seem pretty close. The plane strain condition is used in the remaining two-dimensional studies of the current work.

3.2. Mesh Study

In order to verify the mesh, a mesh study is conducted for two- and three-dimensional problems. The results are tabulated in Table 2. The mesh with 4400 elements and 80000 elements are chosen for two-dimensional and three-dimensional problems, respectively.

Table 2: Mesh study results for two- and three-dimensional problem

Two-dimensional problem Total element number	C_{11}[GPa]	C_{12}[GPa]	Three-dimensional problem Total element number	C_{11}[GPa]	C_{12}[GPa]
1100	7.4432	3.9151	16000	3.5654	1.7943
2504	7.4407	3.9140	57088	3.5648	1.7941
4400	7.4397	3.9136	80000	3.5646	1.7940
6924	7.4392	3.9134	258648	3.5645	1.7939
9900	7.4390	3.9134	432000	3.5644	1.7939

3.3. Dilute limit violation

Higher volume fractions of inclusion and interphase are studied to show the eligibility of the proposed method over the dilute limit. In Fig. 4a, it is observed for the two-dimensional problem that all three models are in good agreement for the stiff interphase case, while for the soft interphase case, the proposed method performs remarkably better than the D-I method. Furthermore, Fig. 4b shows that in three-dimensional problems as the total volume fraction of inclusion and interphase increases, the gap between the reference solution and the proposed method slightly opens for the stiff interphase. On the other hand, no dependency on the volume fraction is observed for the stiff interphase case in two dimensions, see Fig. 4a. Fig. 4b indicates the opposite behavior in three-dimensional problems, i.e., the proposed model works well over dilute limit for the soft interphase case. The discrepancy between the reference solution and the proposed model also slightly increases but it is negligible compared to two-dimensional case. Contrary to the two-dimensional results, the performance of the methods for the stiff interphase case shows a dependency on the volume fraction. It seems that over the dilute limit, the D-I model and the proposed method do not calculate the effective properties very well. The two-level homogenization technique may overestimate the homogenized properties of the multi-phase composite. It is known that the D-I and the M-T methods work better in the volume fraction range of 0% – 30%. For really high volume fractions, micromechanics-based methods such as the D-I and the M-T methods are not very suitable. This may be an explanation for the discrepancy between the D-I method and the reference solution. However, an interesting result is that the proposed two-level homogenization scheme overestimates both the reference and the D-I solutions over the dilute limit. In the stiff interphase case, first level's results, effective inclusion material properties cause the highly stiff behavior for high volume fractions. Fig. 4b demonstrates that the proposed method can be performed for soft interphase with high volume fractions, and calculated effective properties are very close to reference solution. Nevertheless, there may be a slight overestimation for D-I and the proposed model for the stiff interphase case. Comparison with two-dimensions results also indicate that, for soft interphase, the proposed method works better in three dimensions as well for soft interphase.

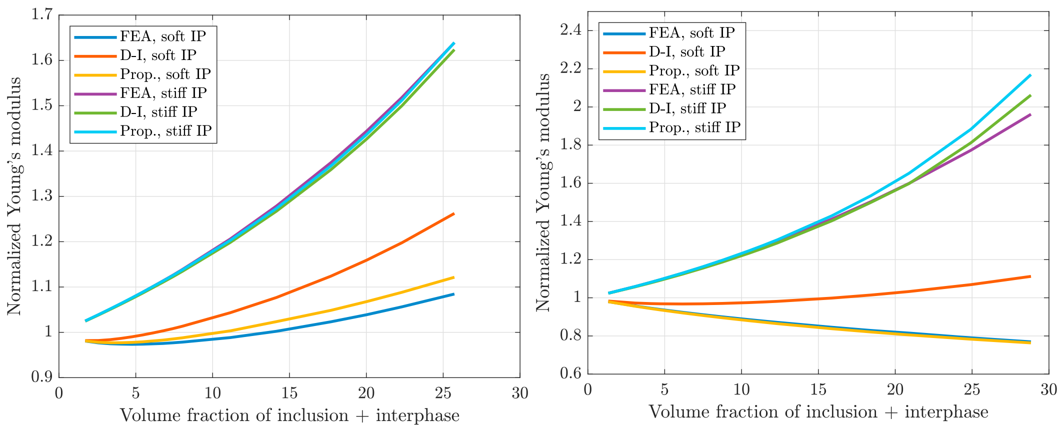

(a) Two-dimensional results (b) Three-dimensional results

Fig. 4: Dilute limit violation for two- and three-dimensional problems

4. Conclusion

In the article, a two-level homogenization method for polymer nanocomposites with coated inclusions is proposed. Depending on the interphase thickness, interphase volume fraction may correspond to a significant portion; hence interphase modeling is essential for polymer nanocomposites.

- When there is soft interphase (softer than the matrix and the inclusion), the load transfer between the matrix and the interphase is prevented. Micromechanics-based *Double-Inclusion* method cannot predict that behavior, as illustrated in Fig. 3b.
- The proposed method provides a remarkable improvement compared to the micromechanics-based method for the soft interphase case, for two-dimensional (circular) and three-dimensional (spherical) RVEs illustrated in Fig. 3d and 3b.
- The proposed methodology is proven to be eligible over the dilute limit for two- and three-dimensional problems.

Acknowledgements

This work is supported by the Scientific and Technological Research Council of Turkey (TUBITAK), Grant No. 218M274.

References

ABAQUS, 2009. ABAQUS/Standard User's Manual, Version 6.9. Dassault Systèmes Simulia Corp, United States.

Benveniste, Y., Dvorak, G., Chen, T., 1989. Stress fields in composites with coated inclusions. Mechanics of Materials 7, 305 – 317.

Bhattacharya, S.N., Kamal, M.R., Gupta, R.K., 2008. Application of polymer nanocomposites, in: Bhattacharya, S.N., Kamal, M.R., Gupta, R.K. (Eds.), Nanocomposites. Hanser, pp. 339 – 373.

Brune, P., Blackman, G., Diehl, T., Meth, J., Brill, D., Tao, Y., Thornton, J., 2016. Direct measurement of rubber interphase stiffness. Macromolecules 49.

Chatzigeorgiou, G., Seidel, G.D., Lagoudas, D.C., 2012. Effective mechanical properties of "fuzzy fiber" composites. Composites Part B: Engineering 43, 2577 – 2593. Homogenization and Micromechanics of Smart and Multifunctional Materials.

Christensen, R., Lo, K., 1979. Solutions for effective shear properties in three phase sphere and cylinder models. Journal of the Mechanics and Physics of Solids 27, 315 – 330.

Eshelby, J.D., 1957. The determination of the elastic field of an ellipsoidal inclusion, and related problems. Proceedings of the Royal Society of London. Series A. Mathematical and Physical Sciences 241, 376–396.

Firooz, S., Saeb, S., Chatzigeorgiou, G., Meraghni, F., Steinmann, P., Javili, A., 2019. Systematic study of homogenization and the utility of circular simplified representative volume element. Mathematics and Mechanics of Solids 24, 2961–2985.

Friebel, C., Doghri, I., Legat, V., 2006. General mean-field homogenization schemes for viscoelastic composites containing multiple phases of coated inclusions. International Journal of Solids and Structures 43, 2513 – 2541.

Güzel, D., 2021. A two-level homogenization method for polymer nanocomposites with coated inclusions. Master's thesis. Middle East Technical University.

Hashin, Z., 1962. The Elastic Moduli of Heterogeneous Materials. Journal of Applied Mechanics 29, 143–150.

Herve, E., Zaoui, A., 1993. n-layered inclusion-based micromechanical modelling. International Journal of Engineering Science 31, 1 – 10.

Hori, M., Nemat-Nasser, S., 1993. Double-inclusion model and overall moduli of multi-phase composites. Mechanics of Materials 14, 189 – 206.

Li, J.Y., 2000. Thermoelastic behavior of composites with functionally graded interphase: a multi-inclusion model. International Journal of Solids and Structures 37, 5579 – 5597.

Mori, T., Tanaka, K., 1973. Average stress in matrix and average elastic energy of materials with misfitting inclusions. Acta Metallurgica 21, 571 – 574.

Odegard, G., Clancy, T., Gates, T., 2005. Modeling of the mechanical properties of nanoparticle/polymer composites. Polymer 46, 553 – 562.

Shajari, A.R., Ghajar, R., Shokrieh, M.M., 2018. Multiscale modeling of the viscoelastic properties of cnt/polymer nanocomposites, using complex and time-dependent homogenizations. Computational Materials Science 142, 395 – 409.

Tian, C., Chu, G., Feng, Y., Lu, Y., Miao, C., Ning, N., Zhang, L., Tian, M., 2019. Quantitatively identify and understand the interphase of sio2/rubber nanocomposites by using nanomechanical mapping technique of afm. Composites Science and Technology 170, 1 – 6.

Wang, Z., Oelkers, R., Lee, K., Fisher, F., 2016. Annular coated inclusion model and applications for polymer nanocomposites – part i: Spherical inclusions. Mechanics of Materials 101, 170 – 184.